LANGMUIR

Biological and Environmental Phenomena at the Interface

Sub-Angstrom Gold Nanoparticle and Liposome Interfaces Controlled by Halides

Xiuru Liu, Xiaoqiu Li, Wu Xu, Xiaohan Zhang, Zhicheng Huang, Feng Wang, and Juewen Liu

Langmuir, **Just Accepted Manuscript** • DOI: 10.1021/acs.langmuir.8b01138 • Publication Date (Web): 09 May 2018

is published by the American Chemical Society. 1155 Sixteenth Street N.W., Washington, DC 20036

Sub-Angstrom Gold Nanoparticle and Liposome Interfaces Controlled by Halides

Xiuru Liu,[1,†] Xiaoqiu Li,[2,†] Wu Xu,[1] Xiaohan Zhang,[3] Zhicheng Huang,[3] Feng Wang,[1,3,*] and Juewen Liu[3,*]

[1] School of Biological and Medical Engineering, Hefei University of Technology, Hefei, Anhui 230009, China.

[2] Center of Intervention Radiology, Center of Precise Medicine, Zhuhai People's Hospital, No.79 Kangning Road, 519000, Zhuhai, Guangdong Province, China.

[3] Department of Chemistry, Waterloo Institute for Nanotechnology, University of Waterloo, Waterloo, Ontario, Canada, N2L 3G1.

[†] X. Liu and X. Li contributed equally to this work.

ABSTRACT. A hallmark of nanoscience is size-dependent and distance-dependent physical properties. While most previous studies focused on optical properties, which are often tuned at nanometer scale, we herein report on the interaction between halide-capped gold nanoparticles (AuNPs) and phosphocholine (PC) liposomes at the sub-Angstrom level. Halide-capped AuNPs are adsorbed by PC liposomes attributable to van der Waals force. Iodide-capped AuNPs interact much more weakly with the liposomes compared to bromide and chloride-capped AuNPs, as indicated by a liposome leakage assay and differential scanning calorimetry. This is explained by the slightly larger size of iodide separating the AuNP core more from the liposome surface. Cryo-TEM indicates the liposomes remain intact when mixed with these halide-capped AuNPs of 13 or 70 nm in diameter. Other even larger ligands, including small thiol compounds, DNA oligonucleotides, proteins and polymers, fully blocked the interaction, while AuNPs dispersed in non-interacting ions including fluoride, phosphate, perchlorate, nitrate, sulfate, and bicarbonate still adsorbed strongly to DOPC liposomes. Taken together, halides can be used to control inter-particle distances at an extremely small scale with remarkable effects over materials properties, allowing surface probing, biosensor development and fundamental surface science studies.

INTRODUCTION

Controlling physical properties of materials as a function of size and distance is a hallmark of nanoscience.[1, 2] To achieve a precise distance control, many methods have been developed. For example, lithography can now reach a resolution of a few nanometers. DNA has a theoretic resolution of a single base pair (~3.4 Å).[2] Atomic force microscopy positions particles even with sub-nm precision. These length scales are useful for probing many interesting phenomena such as plasmonic coupling,[3, 4] fluorescence quenching,[5-7] and electrostatic forces. However, very short-ranged interactions require even finer controlling of distance with a sub-angstrom resolution, which is challenging without highly sophisticated equipment. We are interested in achieving this goal by using chemical methods. For example, attractive van der Waals (VDW) force decays very sharply with distance (r^{-6}), and tuning inter-particle distance might be achieved by adsorption of certain ligands.

Gold nanoparticles (AuNPs) are very interesting for their size and distance dependent optical properties.[8-10] Adjusting the distance between AuNPs produces a visible color change, which can be achieved by thiolated ligands, DNA, and other molecules.[2, 11] While plasmonic coupling of AuNPs is readily observed by tuning inter-particle distance at the nanometer scale,[11, 12] AuNPs might also be useful for probing other properties with an even more sensitive distance-dependent function.

Phosphocholine (PC) lipids have been a subject of extensive studies for fundamental physical sciences, mimicking cell membrane, and device fabrication.[13-18] The structures of DOPC and DPPC lipids are shown in Figure 1A. Their zwitterionic headgroup is overall charge neutral and highly hydrated. PC lipids are the most abundant component of the outer membrane of

eukaryotic cells with excellent anti-fouling property (e.g. resistant to protein adsorption) and biocompatibility. DOPC is in the fluid phase at room temperature, whereas DPPC is in the gel phase with lower lateral diffusion of the lipid chains within the bilayer.

Adsorption of nanoparticles to single-component fluid PC lipid bilayers can result in a local gelation (e.g. a fluid-to-gel phase transition).[19] This has been demonstrated with a diverse range of nanomaterials.[14, 19-23] Among them, AuNPs produced the most drastic effect, including a shifted phase transition temperature (T_c) measurable by differential scanning calorimetry (DSC),[22, 24] which was attributed to the very large Hamaker constant of AuNPs and thus strong VDW attraction to the underneath lipids. VDW force is a short-ranged interaction and it decays quickly with the inter-particle distance (r^{-6}). Therefore, we hypothesize that the interaction strength is a strong function of the distance between AuNPs and the liposome. To observe such a change, however, we need to control the spacing very precisely at very short distances. Herein, we used three halide ions and a few other small molecules as spacers between AuNPs and PC liposomes.

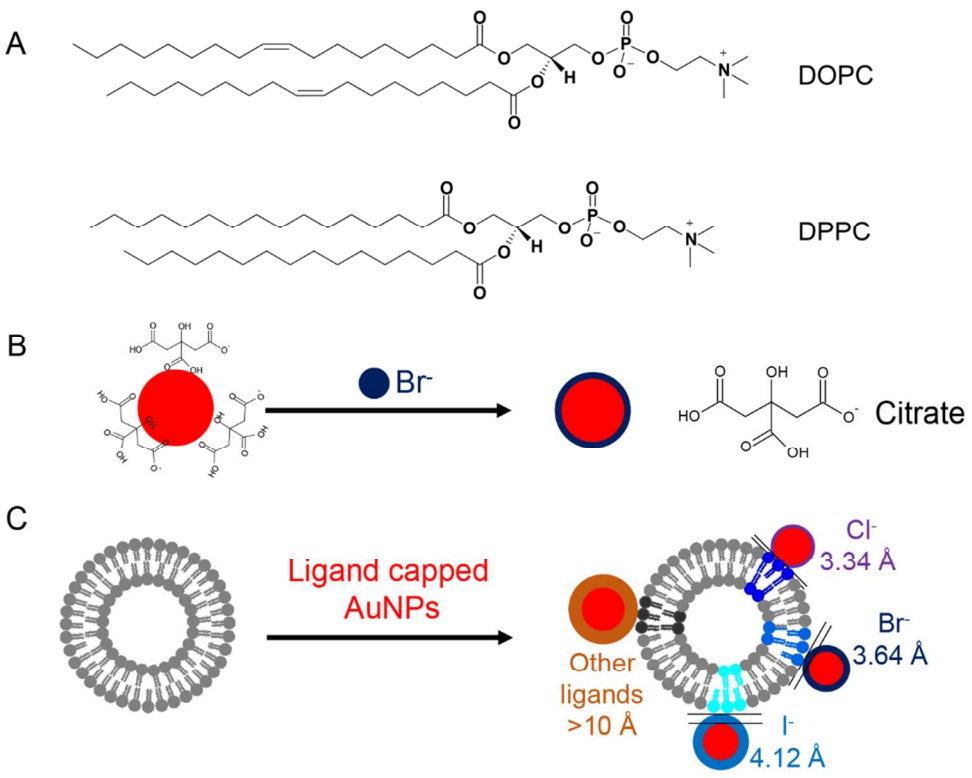

Figure 1. (A) The structures of DOPC and DPPC lipids. (B) Displacing weakly adsorbed citrate by a stronger ligand such as Br^- on the AuNP surface. (C) A scheme of DOPC liposomes adsorbing AuNPs coated with various halides and other ligands. The color-coded lipids indicate different degrees of local lipid phase transition, and the non-adsorbed DOPC lipids are in the fluid phase. The distances between the gold core and the lipid surface are marked in each case based on literature reported size of the halides.

MATERIALS AND METHODS

Chemicals. All the phospholipids were from Avanti Polar Lipids (Alabaster, AL). 4-(2-Hydroxyethyl)-1-piperazineethanesulfonic acid (HEPES), and trisodium citrate and NaCl were from Mandel Scientific (Guelph, ON, Canada). Disodium calcein, $HAuCl_4$, glutathione (GSH),

bovine serum albumin (BSA), 3-mercaptopropionic acid (MPA), sodium fluoride, sodium bromide, sodium iodide, sodium perchlorate, sodium dihydrogen phosphate, sodium nitrate, sodium sulfate, sodium bicarbonate, and Triton X-100 were from Sigma-Aldrich (St Louis, MO). Polyethylene glycol (PEG, MW = 2000) was from Alfa Aesar (Ward Hill, MA). The A_{15} DNA (5′-AAAAAAAAAAAAAAA) was from Integrated DNA Technologies Inc (Coralville, IA). Milli-Q water was used to prepare all the buffers and solutions.

Preparation of liposomes and AuNPs. Liposomes were prepared using the standard extrusion method as described previously.[25] To prepare DOPC liposomes, the dried lipid films were hydrated with 0.5 mL buffer A (100 mM NaCl, 10 mM HEPES, pH 7.4) to reach a final lipid concentration of 5 mg mL^{-1}. The resulting cloudy suspension was extruded through two stacked polycarbonate membrane (pore size = 100 nm) for 21 times. Since DPPC has a T_c of 41 °C, a 65 °C water bath was used to hydrate DPPC with same volume of buffer A. To encapsulate calcein, the dried DOPC lipid film was hydrated with 100 mM disodium calcein solution overnight. After extrusion, free calcein was removed by passing the samples (30 μL) through a Pd-10 column using buffer A for elution, where the first 600 μL of the fluorescent fraction was collected. Citrate-capped 13 nm or 70 nm gold nanoparticles were prepared by chemical reduction of $HAuCl_4$ using citrate as the reducing agent and stabilizer.[26, 27] For the 13 nm AuNPs, $HAuCl_4$ (100 mL, 1 mM) was heated to reflux and then 10 mL of 38.8 mM sodium citrate was added. For the 70 nm AuNPs, 200 mL of 0.3 mM $HAuCl_4$ solution was heated to reflux. Then 1.8 mL of 38.8 mM sodium citrate was added. Their concentrations were estimated to be ~10 nM (for 13 nm) and 0.025 nM (for 70 nm).

Surface modification of AuNPs and characterization. To prepare surface-modified AuNPs, 10 μL NaCl (500 mM), NaBr (500 mM), NaI (100 mM) or MPA (25 mM) was added to 990 μL AuNPs (10 nM) and incubated overnight. The size of these halide-capped AuNPs (10 nM) was characterized using Malvern ZS90 (Malvern Instruments Ltd., England) dynamic light scattering (DLS) with a He-Ne laser (633 nm) at 90° collecting optics. UV-vis absorption spectra of halide-capped AuNPs were obtained in a quartz cuvette using an Agilent 8453A spectrophotometer. TEM measurements were performed on a Philips CM10 transmission electron microscope. The Raman samples were prepared by transferring 20 μL sample solutions on a silicon wafer and the samples were dried overnight. Raman measurements were carried out on a Horiba JY-HR800 spectrometer with a CW 633 nm HeNe excitation source, with a maximum power output of ~1 mW. The spectra were acquired with a 10× objective and laser power of 13 mW before objective. To understand aggregation of AuNPs, 100 μL citrate capped AuNPs (10 nM) was incubated with different final concentrations of NaCl, NaBr or NaI. After 30 min incubation, the samples were photographed using a digital camera.

Cryo-TEM. DOPC liposomes (2 μL, 46 nM or 5 mg/mL) were mixed with 13 nm citrate/AuNPs or 13 nm halide/AuNPs (100 μL, 10 nM) (particle molar ratio 1:10). DOPC (2 μL, 1 nM) liposomes were also mixed with 70 nm AuNPs (100 μL, 0.025 nM) (particle molar ratio 1:1). The samples were then allowed to sit at room temperature for 1 h. Cryo-TEM experiment was performed by spotting the DOPC/AuNP sample (5 μL) on a carbon-coated copper TEM grid (treated with plasma to ensure surface was hydrophilic) in a humidity controlled chamber (FEI Vitrobot). The humidity was set to be 95 to 100% during this operation. The grid was blotted with two filter papers for 2 sec and quickly plunged into liquid ethane. The sample was then

loaded to a liquid N_2 cooled stage at -178 °C and imaged using a 200 kV field emission TEM (FEI Tecnai G2 F20).

Adsorption of AuNPs by liposomes. To understand aggregation of surface-modified AuNPs on liposomes, 2 μL DOPC (5 mg mL^{-1}) was added to 100 μL of citrate (~3 mM), chloride (5 mM), bromide (5 mM) or iodide (1 mM) capped AuNPs (10 nM). After 10 min incubation, the samples was photographed using a digital camera (Canon PowerShot SD 1200 IS). Adsorption of the AuNPs (200 μL, 10 nM) by 1% rhodamine labeled DOPC liposomes (5 mg mL^{-1}) was performed after centrifugation at 12,000 rpm. The supernatant fluorescence proportional to the non-adsorbed liposomes was measured using a Varian Eclipse fluorometer with an excitation wavelength at 560 nm.

Liposome integrity test. To test liposome leakage induced by AuNPs, 5 μL Pd-10 column purified calcein-loaded DOPC liposome (~0.3 nM) were added to 595 μL buffer A in a quartz cuvette. The fluorescence intensity was monitored for ~5 min before 6 μL citrate-AuNPs, Cl^-, Br, I^- capped AuNPs or GSH-AuNPs (10 nM) were added. The fluorescence intensity was monitored for another 20 min before 6 μL GSH (10 mM) was added to remove AuNPs from DOPC. After another 20 min, 10 μL 5% Triton X-100 was added to fully rupture the liposomes. Calcein was excited at 485 nm and the emission fluorescence was monitored at 525 nm using a Varian Eclipse fluorometer.

DSC. To measure the T_c of DPPC/AuNPs, 20 μL DPPC (46 nM, 5 mg mL^{-1}) was mixed with 980 μL 10 nM Cl^-, Br^-, I^- capped AuNPs (molar ratio 1:10 with AuNPs in excess) for 60 min. Free DPPC liposome were also tested. The final DPPC concentration for each mixture was 1 nM. The T_c was investigated using a differential scanning calorimeter (MicroCal VP-DSC). For the

DSC measurement, the sample above was degassed and introduced into DSC sample cell, while the reference cell was filled with Milli-Q water. The sample solutions were scanned from 25 °C to 60 °C at a heating rate of 1 °C min^{-1}.

Test of other capping agents. Various compounds were mixed with AuNPs (10 nM, 100 μL) by adding a final of BSA (1 mg mL^{-1}), A_{15} (2 μM), PEG2K (0.5 mg mL^{-1}), GSH (2 mM), MPA (250 μM), fluoride (5 mM), perchlorate (5 mM), dihydrogen phosphate (5 mM), nitrate (5 mM), sulfate (5 mM) and bicarbonate (5 mM) respectively. The mixtures were incubated for 30 min. All the samples remained red and 2 μL DOPC (5 mg mL^{-1}) were added. All the samples were photographed using the digital camera. Calcein leakage tests were also performed as described above.

RESULTS AND DISCUSSION

Halide-capped AuNPs. We chose halides in this work as a spacer on AuNPs to control the distance between adsorbed liposomes and gold surface. Except for fluoride, most of halide ions have a high affinity towards gold surfaces.[28, 29] Halide-capped AuNPs were prepared by adding the sodium salt of chloride (5 mM), bromide (5 mM) and iodide (1 mM) respectively to citrate-capped AuNPs. A cartoon showing the displacement of citrate by Br^- is shown in Figure 1B. These halide concentrations were chosen to maximally retain the colloidal stability of AuNPs, while further addition of their salts resulted in significant aggregation as indicated by a color change (Figure 2A). Under our conditions, these halide-capped AuNPs remained well dispersed as characterized by dynamic light scattering (DLS, Figure 2C), UV-vis spectroscopy (Figure S1) and transmission electron microscopy (TEM, Figure S2).

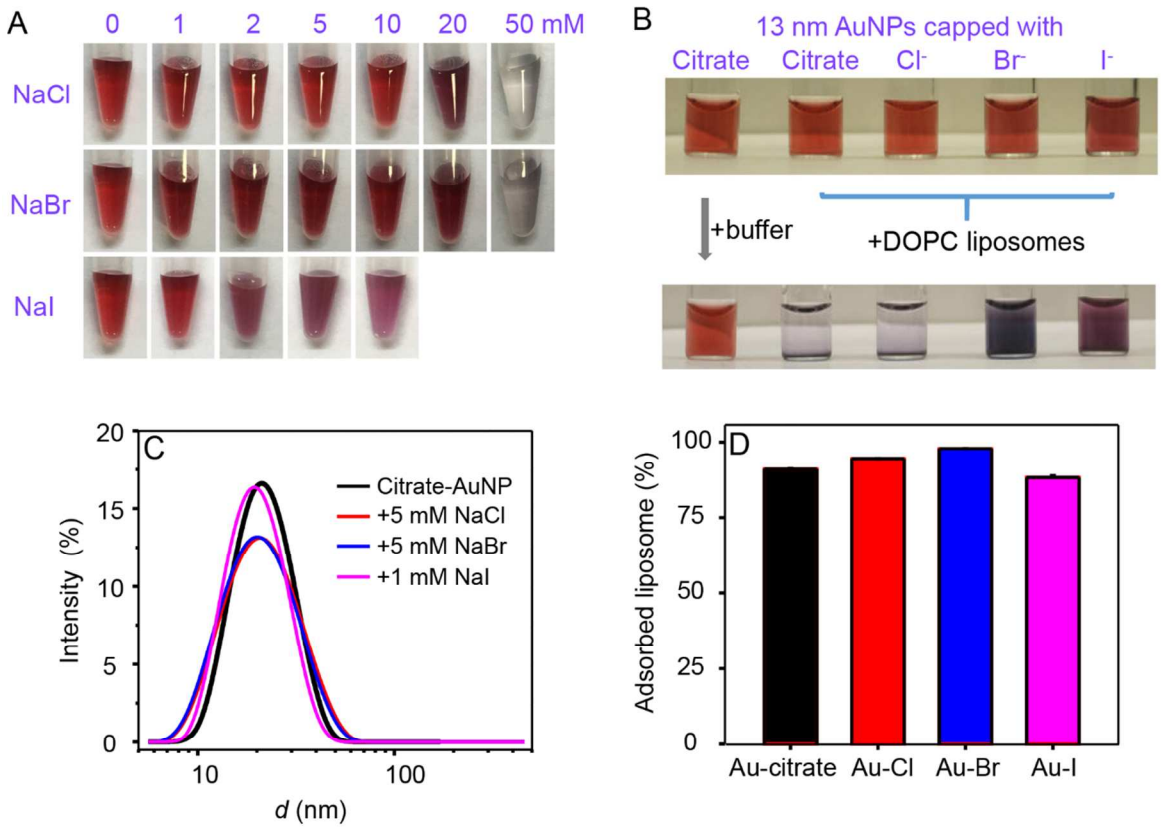

Figure 2. (A) Photographs of 13 nm citrate-capped AuNPs incubated with various concentrations of halides for 6 h. A color change indicated aggregation or etching of AuNPs. (B) Photographs of AuNPs capped by various ligands before and after adding DOPC liposomes. The change of color indicates AuNP adsorption and aggregation on the liposome surface. The buffer control was 2 μL of buffer A into 100 μL of the AuNPs, which had the same salt conentration as for the other samples. (C) Size of citrate and halide-capped AuNPs characterized by DLS. (D) Quantitative analysis of adsorbed liposomes by halide-capped AuNPs. After centrifugation, free non-adsorbed liposomes remained in the supernatant and their fluorescence was measured.

To further confirm the surface chemistry, we then characterized these AuNPs using Raman spectroscopy (Figure 3A). The original citrate-capped AuNPs had a strong Raman peak at 260

cm^{-1}, corresponding to the Au-Cl bond. The chloride source was the $HAuCl_4$ used for the synthesis. We did not observe any citrate related signals from this sample, suggesting that citrate was only loosely associated with the AuNPs without strong chemical interactions.[30, 31] With an additional 5 mM NaCl, the intensity and position of the Au-Cl peak remained the same, suggesting no further Cl^- binding. With the addition of 5 mM NaBr and NaI, the Au-Cl peak disappeared while the Au-Br (187 cm^{-1}) and Au-I (109 cm^{-1}) peaks emerged.[32] This trend is explained by the substitution of surface chloride by bromide and iodide and our data were consistent with the interaction strength of halides with gold following the order of $I^- > Br^- > Cl^-$.[29, 33] This set of experiments indicated that we successfully controlled the surface ligand on the AuNPs.

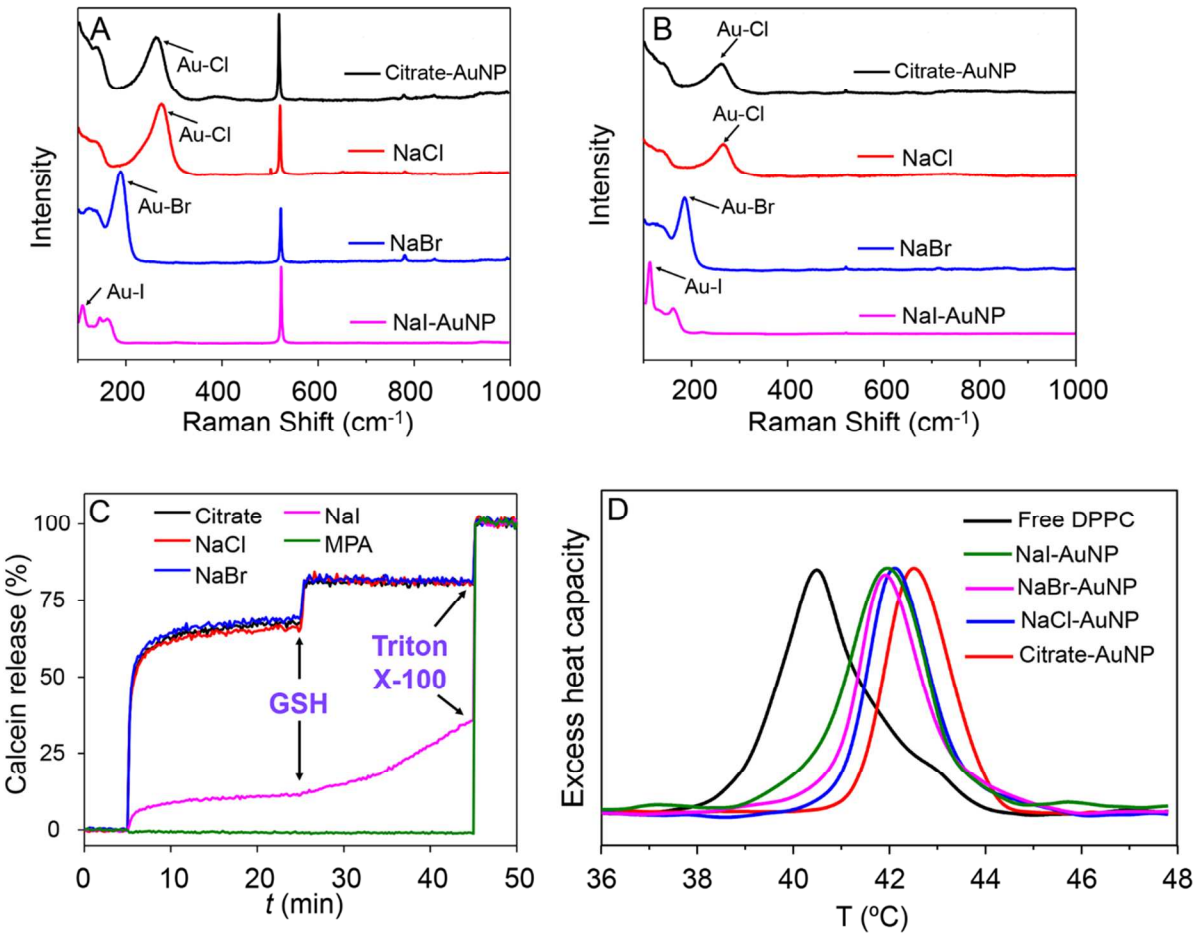

Figure 3. Raman spectra of 13 nm AuNPs capped by various halides of 5 mM (A) before and (B) after mixing with DOPC liposomes. The lack of spectral change after adding DOPC suggests little direct chemical interaction between AuNPs and the lipid headgroup. The sharp peaks in (A) at 520 cm^{-1} were from the silicon wafer substrate, and this peak did not show up in (B) likely due to forming a thicker sample film with the liposomes fully masking the surface. (C) Calcein leakage test of DOPC liposomes after adding various AuNPs. Triton X-100 was finally added to fully rupture the liposomes. (D) DSC traces of DPPC liposomes after mixing with various AuNPs.

Halide-dependent adsorption of AuNPs by DOPC liposomes. The structure of a DOPC lipid is shown in Figure 1A and we prepared its liposomes by the extrusion method with a size of ~100 nm (Figure S3). We then respectively mixed each halide-capped AuNPs with the DOPC liposomes (10 AuNP: 1 liposome, particle number ratio). Before mixing, all these AuNPs were red and well-dispersed (Figure 2B). After mixing, the color of the AuNPs gradually turned purple indicating aggregation. It is interesting that the aggregation was the most extensive for the citrate and Cl^- capped samples, followed by Br^-, while the I^- sample was the least aggregated. Such aggregation was not due to the increased ionic strength since the control sample had the same amount of added salt but no liposome, and it remained red (the first vial in Figure 2B). The color change is explained by the adsorption of AuNPs onto the liposome surface, which further induced aggregation. The reason for such liposome surface induced aggregation was described in previous publications and it was believed to be related to the elimination of lipid gel and fluid phase boundaries (adsorption of AuNPs may cause local gelation of DOPC liposomes).[24, 34, 35]

To further confirm adsorption, we prepared DOPC liposomes with a 1% rhodamine (Rh) label. AuNPs were mixed with the Rh-DOPC at a 43:1 particle number ratio. After mixing, the samples were centrifuged at 15,000 rpm, and we then measured the supernatant fluorescence intensity. Since free liposomes could not be precipitated at this speed, the decreased supernatant fluorescence was attributed to adsorption of the AuNPs. Based on this, citrate-AuNPs, Cl^--, Br^--, I^--AuNPs can all adsorb around 90% Rh-DOPC (Figure 2D).

To understand how the AuNPs were associated with the liposomes, we carried out a cryo-TEM experiment by quickly freezing the mixed samples. For all the Cl^--AuNP (Figure 4A), Br^--AuNP (Figure 4B), and I^--AuNP samples (Figure 4C), the liposome retained a spherical shape and the AuNPs were associated with the liposome surface. Therefore, the AuNPs did not disrupt the liposomes. With the above experiments, we have reached a scheme with simple surface adsorption for these AuNPs (Figure 1C), and the surface ligands on the AuNPs should remain on the surface (vide infra). We also noticed that some Br^- and I^--capped AuNPs formed small aggregates that were not associated with the liposomes (Figure 4B, C). Such moderate aggregation was likely due to the added halide salts and further increase of ionic strength by the buffer from the added liposomes.

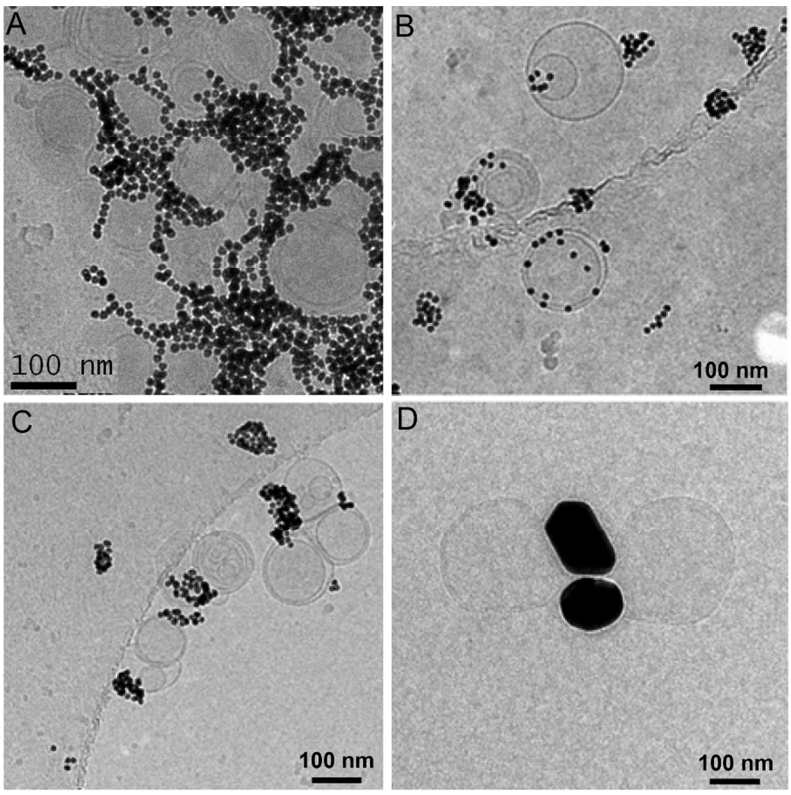

Figure 4. Cryo-TEM micrographs of DOPC liposomes mixed with (A) 13 nm citrate-AuNPs, (B) 13 nm bromide-AuNPs, (C) 13 nm iodide-AuNPs, and (D) 70 nm citrate-AuNPs.

Halide-dependent interaction strength. After confirming adsorption, we then wanted to study the interaction strength in each case. A more strongly adsorbed AuNP might produce a more drastic change in the packing of the underlying lipid molecules, and thus affect the lipid phase transition more.[19, 22] For this purpose, we first performed a liposome leakage assay. Around 100 mM calcein was encapsulated in the DOPC liposomes to reach self-quenching concentration and free calcein was removed. In this case, if the liposome leaks, we expect to observe fluorescence enhancement. The fluorescence of the liposome was monitored as a function of time (Figure 3C). The background fluorescence was flat for all the samples, suggesting that the liposomes were stable and free of leakage. At 5 min, a small volume of AuNP solution was added and we

observed an obvious fluorescence increase for the citrate, Cl^- and Br^- capped AuNPs, while the I^- coated AuNPs showed a much lower response. Since we already knew that the liposome structure was retained from cryo-TEM, such leakage was attributed only to local defects instead of rupture of the liposomes.

A liposome leaks its content the fastest at its T_c.[36] Since DOPC has a T_c of -20 °C, it is in the fluid phase at room temperature. Therefore, our leakage is attributed to adsorption induced by the fluid-to-gel phase transition of the liposome at the spot of adsorption.[19, 22] After adsorption, the phase transition was complete and the liposome became stable again. A further line of evidence was that leakage also occurred at 25 min, at which GSH (a thiol containing peptide) was added to remove the adsorbed AuNPs from the liposome surface. Since thiol has higher affinity than halides for a gold surface, GSH coated the AuNPs and reduced their affinity to the DOPC liposomes. In this case, the liposomes underwent a gel-to-fluid phase transition, which also caused a transient leakage.[22] In the end, Triton X-100 was added at 45 min to fully rupture the liposomes so that the fraction of leakage at each step could be calculated. These experiments suggest that the iodide-capped AuNPs had the weakest interaction with the DOPC liposome among the four types of AuNPs tested.

To further measure the interaction strength, a differential scanning calorimetry (DSC) experiment was performed (Figure 3D). Since the DOPC lipid has a T_c of -20 °C, we cannot measure it directly in the aqueous solution. We used its saturated counterpart DPPC (T_c = 41 °C) for this experiment. The AuNP/liposome mixtures were dispersed in buffer and temperature was gradually raised. The free DPPC liposomes indeed had a peak at 41 °C. In the presence of AuNPs, all the samples showed a higher T_c value, while the largest shift occurred with citrate-

capped AuNPs and the smallest shift with iodide-capped ones. This also indicates a weaker interaction with the iodide-coated AuNPs.

Discussion of surface forces. So far, we observed that iodide-capped AuNPs interacted with PC liposomes much more weakly compared to the bromide and chloride capped ones. Now, we want to explain this difference. First, we tested whether AuNPs and DOPC liposomes have direct chemical interactions. We measured the Raman spectra of these AuNPs after mixing them with DOPC liposomes (Figure 3B). In each case, the Au-halide bond remained intact and we did not observe any new peak responsible for the Au-DOPC interaction. From the chemistry standpoint, the PC headgroup is a poor ligand for AuNPs. Therefore, direct chemical bonding between AuNP and the lipid headgroup was absent and the PC headgroup was unable to displace even the weakest chlorides on AuNPs. Therefore, the halide shell on AuNPs separated the AuNP core from the liposome surface as depicted in Figure 1C.

After ruling out direct chemical interactions, we then analyzed electrostatic interactions. All the halide-capped AuNPs are negatively charged, and the PC headgroup is zwitterionic and thus charge neutral. Therefore, electrostatic attraction is unlikely to happen or make a large difference among these AuNPs. Hydrophobic interaction is also unlikely since the PC headgroup is extremely hydrophilic and hydrated.[37] We reason that the VDW forces are the main interaction force, and previous studies also supported this.[22, 24] Coating a layer of iodide might have increased the distance between the AuNP and liposome, thus weakening the VDW force.

AuNPs are especially effective for VDW interactions since they have a very large Hamaker constant. For example, the VDW force between gold is nearly 90-fold times stronger than that between polystyrene.[38] Indeed, most other nanomaterials such as latex beads,[20, 21, 39] highly

oxidized graphene oxide, nanodiamond, and carbon nanotubes did not induce liposome leakage,[40, 41] which is likely due to their weaker VDW interaction with the liposome being insufficient to cause the needed extent of phase transition.

Coating AuNPs with other larger ligands. The above studies focused on a few halides that are known to adsorb strongly on a gold surface. To further confirm our hypothesis, we tested a few more anions and molecules. First, small anions such as fluoride, perchlorate, dihydrogen phosphate, nitrate, sulfate and bicarbonate are known to interact poorly with AuNPs. With these ions, the AuNPs behaved just like citrate-capped AuNPs to be aggregated by DOPC liposomes (Figure 5A) and induced its leakage (Figure 5C, solid lines). On the other hand, strong ligands such as MPA, GSH, DNA, BSA and even weak PEG inhibited the aggregation (Figure 5B) and no liposome leakage was observed (Figure 5C, dashed lines). Compared to iodide, these ligands are much larger and they separated the AuNP core from the liposome surface even further. This led to a poor VDW force. It is interesting to note that even PEG can inhibit the interaction.

So far, we have demonstrated the control of AuNP and PC liposome interactions by various halides. The diameter of an I^- ion is just 4.12 Å, which is only 0.48 Å larger than that of Br^-. Both Br^- and I^- are strong ligands for gold, while adsorption of Cl^- is weaker.[28, 33, 42, 43] The drastic difference between Br^- and I^- also supports the effect of halide size, and a threshold is crossed between Br^- and I^-. Note that iodide-capped AuNPs still interact quite strongly with the liposome, since a small amount of leakage and AuNP color change were still observed. A slightly larger ligand such as MPA fully inhibited these reactions (Figure 5B, 5C). Since our measurements could not directly give the interaction force, no quantitative calculations were made, but it is likely that halides are a useful method for tuning the distance of AuNPs.

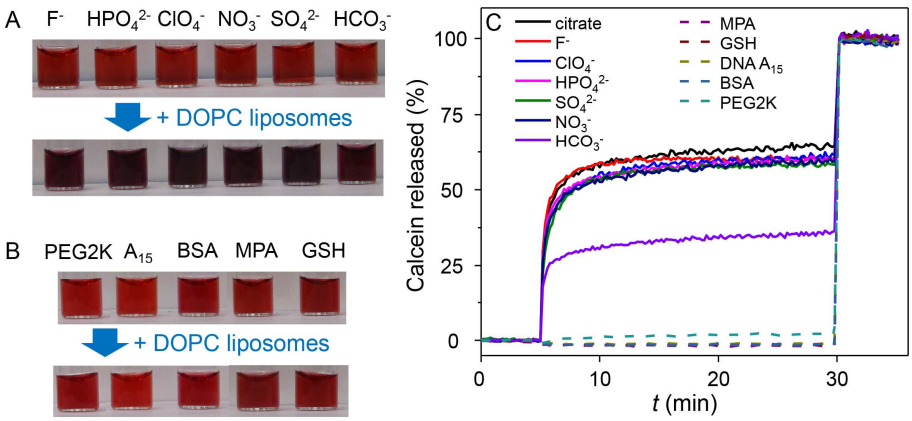

Figure 5. Photographs of 13 nm citrate-capped AuNPs mixed with DOPC liposomes in the presence of (A) various non-adsorbing anions; and (B) molecules that are adsorbed by AuNPs. (C) Calcein leakage kinetics from DOPC liposomes induced by AuNPs in the presence of these anions and molecules. AuNPs were added at 5 min and Triton X-100 was added at 30 min.

Test of larger AuNPs. With a strong VDW interaction, the adsorbed AuNPs may further form supported lipid bilayers. A good example is the fusion of PC liposome with a silica surface, where VDW force is also believed to be responsible for the interaction.[15, 16, 18, 44] In our cryo-TEM with 13 nm AuNPs, however, we did not see such structures and the liposomes remained intact (Figure 4A-C). Such simple adsorption was also observed by others.[34] Many studies have indeed reported on AuNP supported lipid bilayers, but they were not prepared by a simple mixing with PC liposomes in an aqueous solution. Either the liposome or other components have to be cationic, or it requires co-extrusion or freeze-thawing cycles.[45-48] Even on a planar gold surface, to form supported lipid bilayers, the surface needs to be modified.[49] Based on our knowledge, no one has demonstrated direct formation of supported PC bilayers on AuNPs. We also tested 70 nm citrate-capped AuNPs (Figure 4D) and iodide-capped AuNPs (Figure S4) to ensure that the high curvature of small AuNPs was not the reason to inhibit the fusion of

liposome on the AuNPs. In both cases, we still observed intact liposomes. It might be that other factors, such as hydration, are also important to form supported bilayers.[14, 15, 18, 50, 51]

CONCLUSIONS

In summary, we achieved the following important insights from this work. We controlled the interaction between AuNPs and liposomes by coating the gold surface with various halides. Our data suggest that it is the size of halides that affected its VDW interaction strength, which was reflected from leakage of DOPC liposomes and phase transition properties. This work has extended the distance-dependent property of AuNPs beyond its plasmonic and fluorescence quenching behavior. With liposome leakage assays, and liposome induced AuNP aggregation, we can readily probe such short-ranged VDW forces related to AuNPs. Our study suggested it might be possible to use DOPC liposomes to probe the surface ligands on AuNPs in terms of interaction strength and size.

ASSOCIATED CONTENT

Supporting Information. UV-Vis, TEM and cryo-TEM of halide-capped AuNPs, and DLS of DOPC and DPPC liposomes. This material is available free of charge via the Internet at http://pubs.acs.org. (PDF)

AUTHOR INFORMATION

Corresponding Author

*E-mail: fengw420@hfut.edu.cn

*E-mail: liujw@uwaterloo.ca

Notes

The authors declare no competing financial interest.

ACKNOWLEDGMENT

We thank Robert Harris at the University of Guelph for assistance with cryo-TEM. Funding for this work is from the National Natural Science Foundation of China (31571023, 81501587), the Fundamental Research Funds for the Central Universities of China (Grant No. JZ2017HGPA0164) and the Natural Sciences and Engineering Research Council of Canada (NSERC).

REFERENCES

(1) Chen, C. C.; Herhold, A. B.; Johnson, C. S.; Alivisatos, A. P., Size Dependence of Structural Metastability in Semiconductor Nanocrystals. *Science* **1997**, 276, 398-401.

(2) Jones, M. R.; Seeman, N. C.; Mirkin, C. A., Programmable Materials and the Nature of the DNA Bond. *Science* **2015**, 347, 1260901.

(3) Zheng, X.; Liu, Q.; Jing, C.; Li, Y.; Li, D.; Luo, W.; Wen, Y.; He, Y.; Huang, Q.; Long, Y.-T.; Fan, C., Catalytic Gold Nanoparticles for Nanoplasmonic Detection of DNA Hybridization. *Angew. Chem., Int. Ed.* **2011**, 50, 11994-11998.

(4) Shi, L.; Jing, C.; Ma, W.; Li, D. W.; Halls, J. E.; Marken, F.; Long, Y. T., Plasmon Resonance Scattering Spectroscopy at the Single-Nanoparticle Level: Real-Time Monitoring of a Click Reaction. *Angew. Chem. Int. Ed.* **2013**, 52, 6011-6014.

(5) Yun, C. S.; Javier, A.; Jennings, T.; Fisher, M.; Hira, S.; Peterson, S.; Hopkins, B.; Reich, N. O.; Strouse, G. F., Nanometal Surface Energy Transfer in Optical Rulers, Breaking the FRET Barrier. *J. Am. Chem. Soc.* **2005**, 127, 3115-3119.

(6) Huang, P.-J. J.; Liu, J., DNA-Length-Dependent Fluorescence Signaling on Graphene Oxide Surface. *Small* **2012**, 8, 977-983.

(7) Chen, Y.; O'Donoghue, M. B.; Huang, Y.-F.; Kang, H.; Phillips, J. A.; Chen, X.; Estevez, M. C.; Yang, C. J.; Tan, W., A Surface Energy Transfer Nanoruler for Measuring Binding Site Distances on Live Cell Surfaces. *J. Am. Chem. Soc.* **2010**, 132, 16559-16570.

(8) Daniel, M.-C.; Astruc, D., Gold Nanoparticles: Assembly, Supramolecular Chemistry, Quantum-Size-Related Properties, and Applications toward Biology, Catalysis, and Nanotechnology. *Chem. Rev.* **2004**, 104, 293-346.

(9) Zhao, W.; Brook, M. A.; Li, Y., Design of Gold Nanoparticle-Based Colorimetric Biosensing Assays. *ChemBioChem* **2008**, 9, 2363-2371.

(10) Song, S. P.; Qin, Y.; He, Y.; Huang, Q.; Fan, C. H.; Chen, H. Y., Functional Nanoprobes for Ultrasensitive Detection of Biomolecules. *Chem. Soc. Rev.* **2010**, 39, 4234-4243.

(11) Rosi, N. L.; Mirkin, C. A., Nanostructures in Biodiagnostics. *Chem. Rev.* **2005**, 105, 1547-1562.

(12) Fang, L.; Wang, Y.; Liu, M.; Gong, M.; Xu, A.; Deng, Z., Dry Sintering Meets Wet Silver-Ion "Soldering": Charge-Transfer Plasmon Engineering of Solution-Assembled Gold Nanodimers from Visible to near-Infrared I and II Regions. *Angew. Chem., Int. Ed.* **2016**, 55, 14296-14300.

(13) Nel, A. E.; Madler, L.; Velegol, D.; Xia, T.; Hoek, E. M. V.; Somasundaran, P.; Klaessig, F.; Castranova, V.; Thompson, M., Understanding Biophysicochemical Interactions at the Nano-Bio Interface. *Nat. Mater.* **2009**, 8, 543-557.

(14) Liu, J., Interfacing Zwitterionic Liposomes with Inorganic Nanomaterials: Surface Forces, Membrane Integrity, and Applications. *Langmuir* **2016**, 32, 4393-4404.

(15) Castellana, E. T.; Cremer, P. S., Solid Supported Lipid Bilayers: From Biophysical Studies to Sensor Design. *Surf. Sci. Rep.* **2006**, 61, 429-444.

(16) Parikh, A. N.; Groves, J. T., Materials Science of Supported Lipid Membranes. *MRS Bull* **2006**, 31, 507-512.

(17) Liu, Y.; Wang, F.; Liu, J., Headgroup Inversed Liposomes: Biointerfaces, Supported Bilayers and Applications. *Langmuir* **2018**, DOI: 10.1021/acs.langmuir.7b04369.

(18) Cremer, P. S.; Boxer, S. G., Formation and Spreading of Lipid Bilayers on Planar Glass Supports. *J. Phys. Chem. B* **1999**, 103, 2554-2559.

(19) Wang, B.; Zhang, L. F.; Bae, S. C.; Granick, S., Nanoparticle-Induced Surface Reconstruction of Phospholipid Membranes. *Proc. Natl. Acad. Sci. U.S.A.* **2008**, 105, 18171-18175.

(20) Yu, Y.; Anthony, S. M.; Zhang, L. F.; Bae, S. C.; Granick, S., Cationic Nanoparticles Stabilize Zwitterionic Liposomes Better Than Anionic Ones. *J. Phys. Chem. C* **2007**, 111, 8233-8236.

(21) Zhang, L. F.; Granick, S., How to Stabilize Phospholipid Liposomes (Using Nanoparticles). *Nano Lett.* **2006**, 6, 694-698.

(22) Wang, F.; Liu, J., Self-Healable and Reversible Liposome Leakage by Citrate-Capped Gold Nanoparticles: Probing the Initial Adsorption/Desorption Induced Lipid Phase Transition. *Nanoscale* **2015**, 7, 15599-15604.

(23) Liu, Y.; Liu, J., Adsorption of Nanoceria by Phosphocholine Liposomes. *Langmuir* **2016**, 32, 13276-13283.

(24) Wang, F.; Curry, D. E.; Liu, J., Driving Adsorbed Gold Nanoparticle Assembly by Merging Lipid Gel/Fluid Interfaces. *Langmuir* **2015**, 31, 13271-13274.

(25) Wang, F.; Liu, B.; Ip, A. C. F.; Liu, J., Orthogonal Adsorption onto Nano-Graphene Oxide Using Different Intermolecular Forces for Multiplexed Delivery. *Adv. Mater.* **2013**, 25, 4087-4092.

(26) Storhoff, J. J.; Elghanian, R.; Mucic, R. C.; Mirkin, C. A.; Letsinger, R. L., One-Pot Colorimetric Differentiation of Polynucleotides with Single Base Imperfections Using Gold Nanoparticle Probes. *J. Am. Chem. Soc.* **1998**, 120, 1959-1964.

(27) Liu, J.; Lu, Y., Colorimetric Cu^{2+} Detection with a Ligation DNAzyme and Nanoparticles. *Chem. Commun.* **2007**, 4872-4874.

(28) Magnussen, O. M., Ordered Anion Adlayers on Metal Electrode Surfaces. *Chem. Rev.* **2002**, 102, 679-726.

(29) Liu, B.; Wu, P.; Huang, Z.; Ma, L.; Liu, J., Bromide as a Robust Backfiller on Gold for Precise Control of DNA Conformation and High Stability of Spherical Nucleic Acids. *J. Am. Chem. Soc.* **2018**, 140, 4499–4502.

(30) Al-Johani, H.; Abou-Hamad, E.; Jedidi, A.; Widdifield, C. M.; Viger-Gravel, J.; Sangaru, S. S.; Gajan, D.; Anjum, D. H.; Ould-Chikh, S.; Hedhili, M. N.; Gurinov, A.; Kelly, M. J.; El

Eter, M.; Cavallo, L.; Emsley, L.; Basset, J.-M., The Structure and Binding Mode of Citrate in the Stabilization of Gold Nanoparticles. *Nat Chem* **2017**, 9, 890–895.

(31) Park, J.-W.; Shumaker-Parry, J. S., Structural Study of Citrate Layers on Gold Nanoparticles: Role of Intermolecular Interactions in Stabilizing Nanoparticles. *J. Am. Chem. Soc.* **2014**, 136, 1907-1921.

(32) Perera, G. S.; Yang, G.; Nettles, C. B.; Perez, F.; Hollis, T. K.; Zhang, D., Counterion Effects on Electrolyte Interactions with Gold Nanoparticles. *J. Phys. Chem. C* **2016**, 120, 23604-23612.

(33) Lipkowski, J.; Shi, Z.; Chen, A.; Pettinger, B.; Bilger, C., Ionic Adsorption at the Au(111) Electrode. *Electrochimica Acta* **1998**, 43, 2875-2888.

(34) Sugikawa, K.; Kadota, T.; Yasuhara, K.; Ikeda, A., Anisotropic Self-Assembly of Citrate-Coated Gold Nanoparticles on Fluidic Liposomes. *Angew. Chem., Int. Ed.* **2016**, 55, 4059-4063.

(35) Pornpattananangkul, D.; Olson, S.; Aryal, S.; Sartor, M.; Huang, C.-M.; Vecchio, K.; Zhang, L., Stimuli-Responsive Liposome Fusion Mediated by Gold Nanoparticles. *ACS Nano* **2010**, 4, 1935-1942.

(36) Hays, L. M.; Crowe, J. H.; Wolkers, W.; Rudenko, S., Factors Affecting Leakage of Trapped Solutes from Phospholipid Vesicles During Thermotropic Phase Transitions. *Cryobiology* **2001**, 42, 88-102.

(37) Schlenoff, J. B., Zwitteration: Coating Surfaces with Zwitterionic Functionality to Reduce Nonspecific Adsorption. *Langmuir* **2014**, 30, 9625-9636.

(38) Israelachvili, J. N., *Intermolecular and Surface Forces,* 3 ed.; Academic Press: New York, 2011.

(39) Gao, W.; Hu, C.-M. J.; Fang, R. H.; Zhang, L., Liposome-Like Nanostructures for Drug Delivery. *J. Mater. Chem. B* **2013**, 1, 6569-6585.

(40) Ip, A. C. F.; Liu, B.; Huang, P.-J. J.; Liu, J., Oxidation Level-Dependent Zwitterionic Liposome Adsorption and Rupture by Graphene-Based Materials and Light-Induced Content Release. *Small* **2013**, 9, 1030-1035.

(41) Wang, F.; Liu, J., Nanodiamond Decorated Liposomes as Highly Biocompatible Delivery Vehicles and a Comparison with Carbon Nanotubes and Graphene Oxide. *Nanoscale* **2013**, 5, 12375-12382.

(42) Meena, S. K.; Celiksoy, S.; Schafer, P.; Henkel, A.; Sonnichsen, C.; Sulpizi, M., The Role of Halide Ions in the Anisotropic Growth of Gold Nanoparticles: A Microscopic, Atomistic Perspective. *Phys. Chem. Chem. Phys.* **2016**, 18, 13246-13254.

(43) Langille, M. R.; Personick, M. L.; Zhang, J.; Mirkin, C. A., Defining Rules for the Shape Evolution of Gold Nanoparticles. *J. Am. Chem. Soc.* **2012**, 134, 14542-14554.

(44) Mornet, S.; Lambert, O.; Duguet, E.; Brisson, A., The Formation of Supported Lipid Bilayers on Silica Nanoparticles Revealed by Cryoelectron Microscopy. *Nano Lett.* **2005**, 5, 281-285.

(45) Zhang, L.; Li, P.; Li, D.; Guo, S.; Wang, E., Effect of Freeze−Thawing on Lipid Bilayer-Protected Gold Nanoparticles. *Langmuir* **2008**, 24, 3407-3411.

(46) Tam, N. C. M.; Scott, B. M. T.; Voicu, D.; Wilson, B. C.; Zheng, G., Facile Synthesis of Raman Active Phospholipid Gold Nanoparticles. *Bioconjug. Chem.* **2010**, 21, 2178-2182.

(47) Gao, W.; Hu, C.-M. J.; Fang, R. H.; Luk, B. T.; Su, J.; Zhang, L., Surface Functionalization of Gold Nanoparticles with Red Blood Cell Membranes. *Adv. Mater.* **2013**, 25, 3549-3553.

(48) Bailey, C. M.; Kamaloo, E.; Waterman, K. L.; Wang, K. F.; Nagarajan, R.; Camesano, T. A., Size Dependence of Gold Nanoparticle Interactions with a Supported Lipid Bilayer: A QCM-D Study. *Biophys. Chem.* **2015**, 203–204, 51-61.

(49) Sun, W.; Kewalramani, S.; Hujsak, K.; Zhang, H.; Bedzyk, M. J.; Dravid, V. P.; Thaxton, C. S., Mesophase in a Thiolate-Containing Diacyl Phospholipid Self-Assembled Monolayer. *Langmuir* **2015**, 31, 3232-3241.

(50) Reimhult, E.; Hook, F.; Kasemo, B., Intact Vesicle Adsorption and Supported Biomembrane Formation from Vesicles in Solution: Influence of Surface Chemistry, Vesicle Size, Temperature, and Osmotic Pressure *Langmuir* **2003**, 19, 1681-1691.

(51) Richter, R. P.; Berat, R.; Brisson, A. R., Formation of Solid-Supported Lipid Bilayers: An Integrated View. *Langmuir* **2006**, 22, 3497-3505.

For Table of Content Graphics Only